Appl Phys B (2010) 100: 933–943
DOI 10.1007/s00340-010-4135-2

Applied Physics B
Lasers and Optics

Quantitative measurement of naphthalene in low-pressure flames by jet-cooled laser-induced fluorescence

M. Wartel · J.-F. Pauwels · P. Desgroux · X. Mercier

Received: 15 December 2009 / Revised version: 16 June 2010 / Published online: 21 July 2010

Abstract We have recently developed a new laser based set-up (Jet-Cooled Laser-Induced Fluorescence) for the analysis of aromatic compounds generated in flames. This method relies on the extraction of the species from the flame via a thin microprobe and their direct analysis inside a supersonic free jet by Laser-Induced Fluorescence (LIF). Under the supersonic conditions of the jet, the vibronic spectra of the molecules become structured as the possibility of electronic transitions is reduced, allowing their selective detection by LIF. In addition, due to the very low quenching efficiency inside the jet, LIF signals can be directly related to the population of the probed species and easily calibrated into absolute concentrations. All of the work presented here has been carried out for naphthalene, which is an important PAH involved in soot formation mechanisms. The calibration procedure is described in detail. We also report a detailed study of the quantitative features of the technique, in particular cooling efficiencies and collision rates as well as some additional potential factors that could bias the quantitative aspect of the method. Finally, the possibilities of the technique for the measurement of PAH within flames in the presence of soot particles along with its accuracy and reproducibility are demonstrated by recording naphthalene mole fractions profiles in several rich $CH_4/O_2/N_2$ flames. A detection limit of the order of a ppb is demonstrated under flame conditions with and without the presence of soot particles.

M. Wartel · J.-F. Pauwels · P. Desgroux · X. Mercier (✉)
Physicochimie des Processus de Combustion et de l'Atmosphère (PC2A), UMR/CNRS 8522, Fédération de Recherche "Centre d'Etudes et de Recherches Lasers et Applications" (FR 2416), Université de Lille, 59655 Villeneuve d'Ascq Cedex, France
e-mail: xavier.mercier@univ-lille1.fr
Fax: +33-3-20436977

1 Introduction

The understanding of soot formation in flames has been considerably improved in recent decades thanks to the large amount of experimental and modeling work undertaken on the subject. It is now well established that polycylic aromatic hydrocarbons (PAHs) significantly contribute to the formation of primary soot particles [1, 2]. Numerous experimental studies have been performed at atmospheric pressure and have detailed the structure of sooting flames by providing the profiles of a number of gaseous soot precursors and soot particles [3, 4]. To date, the detailed processes involved in the early stages of soot formation are not well understood.

Recent advances in laser diagnostics enable the detection of gaseous soot precursors in the narrow zone where soot inception occurs. Low-pressure premixed flames, in which the reaction zone is a few millimeters wide and well separated from the burner surface, offer an ideal experimental platform for such investigations.

In our laboratory we have recently begun long-term work on soot formation in low-pressure methane/oxygen/nitrogen flames [5]. Methane has been selected because of its important use in domestic and industrial burners. However, while chemical mechanisms of methane oxidation have been the subject of much work even under rich conditions, very few reports on PAHs and soot formation are available, except at atmospheric pressure or above [6, 7]. As the propensity of methane to produce soot is much less than the more commonly studied fuels (acetylene or ethylene), experimental strategies had to be selected to obtain a good signal to noise ratio. A novel experimental set-up, based on calibrated laser-induced fluorescence (LIF) inside an expanded free jet has been developed to obtain quantitative measurements of aromatic compounds after their extraction with a microprobe from the flame. The potential of the technique has been

demonstrated by achieving spatially-resolved benzene profiles in low-pressure flames of various equivalence ratios [8].

In this paper we report a comprehensive study to demonstrate the capabilities of this new set-up to perform quantitative PAH measurements in flames. We focused our work on the naphthalene molecule, which is a key species in soot formation processes. We then present quantitative profiles of naphthalene which have been measured in different methane non-sooting and sooting flames (equivalence ratios from 1.82 to 2.32). From these experiments, it appears that the method allows naphthalene detection with an excellent sensitivity (a few ppb) even in the presence of soot particles. As expected, experimental profiles highlight a strong dependence on the equivalence ratio and their global shapes are similar to the benzene profiles determined previously [8].

2 Experimental set-up

A schematic representation of the experimental set-up is reported in Fig. 1.

2.1 Optical setup

The set-up is nearly the same as reported previously [8], and so only the main details will be given here. The laser system consists of a Quantel Nd:YAG laser, pumping a dye laser (TDL70 Quantel). We used the 2nd harmonic at 532 nm to excite a mixture of Rodamine 640 and DCM in order to generate a tuneable laser pulse around 308 nm after frequency doubling. The beam was sent into the analysis chamber unfocused and spatially reduced (diameter approximately 1 mm) with a pinhole. The laser energy has been adjusted to approximately 0.04 J/cm^2 to be in the linear regime of fluorescence. Fluorescence signals were recorded *via* an Acton 2500i spectrometer (500 mm focal length—gratings with 1200 g/mm or 300 g/mm) which can be coupled either to a 16 bit intensified CCD camera (Roper Pimax II) or to a photomultiplier (Photonis XP2020Q, spectral range 150–650 nm and maximum sensitivity around 420 nm). In this study, we essentially used the camera to record resolved fluorescence spectra and check for the absence of spectral interference along the flame height. The photomultiplier was used to record excitation spectra, to measure the fluorescence decay times and to determine the mole fraction profiles of naphthalene in the different flames. Data points corresponding to these profiles have been determined by integrating the respective temporal LIF signals rather than measuring the maximum voltage values in order to optimize the signal to noise ratio.

2.2 Low-pressure burner and microprobe

The burner used was a flat-flame burner (6 cm diameter), provided by *Holthuis & Associates* [9]. This burner produces stable, flat flames under a wide range of low pressures (approximately from 10 to 300 torr). Flame conditions were characterized by an equivalence ratio of between 1.82 and 2.32 stabilized at a pressure of 200 torr. Flames with an equivalence ratio of greater than 2.05 were determined to be sooting flames. The sampling system consists of a microprobe (extraction diameter around 300 microns) through which the species are extracted from the flame and directly sent into the analysis chamber. This diameter has been chosen, as explained in [8], as it was a good compromise between the requirements of spatial resolution and the propensity of the microprobe to become clogged. The vertical position of the burner can be altered while the position of the microprobe is fixed above it, thus enabling extraction of gaseous samples from the flames all along the flame height. As a result, it is possible to probe the flame and determine mole fraction profiles of naphthalene from 1 to 50 mm above the burner. The microprobe is connected to the analysis chamber *via* a Teflon line, inside which the pressure is kept constant at 10 torr, and which is heated to 100°C in order to avoid condensation of the species. Condensation along the sampling line is one of the main problems encountered when using sampling methods, which generally require a few hundreds torr of gas sample to work properly.

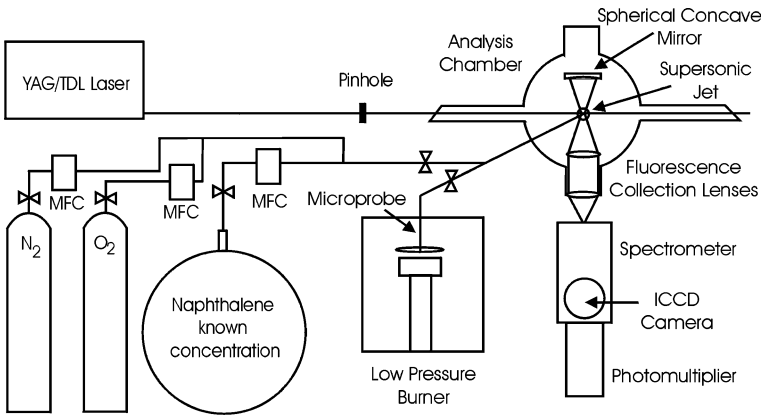

Fig. 1 Experimental set-up

It is therefore necessary to significantly heat the line, typically to greater than 300°C, in order to limit this problem as condensation of a species is directly dependent on its vapor pressure, which is a function of the temperature. The value of the vapor pressure of naphthalene to condensate can be estimated to be greater than 26 torr at 100°C [10]. This is thus even larger than the total pressure of 10 torr within the sampling line. This ensures so the absence of condensation of naphthalene during experiments along the transfer line.

These specific features (low pressure of sampled gas inside the transfer line) could be of great interest to facilitate the study of larger PAH in flames. If we consider e.g., coronene (300 amu) formed in a flame with an estimated mole fraction lower than 1 ppm, its vapor pressure would be around 10^{-5} torr within the sampling line and thus would only require heating the line to approximately 150°C to avoid condensation [11].

An additional important point concerning the sampling line is that it also allows the thermalization of the species before their cooling inside the analysis chamber. This thermalization is essential to guarantee an appreciable and identical cooling of the species inside the expanded free jet whatever their sampling height in the flame. Obviously, only stable species can be analyzed with this sampling procedure, which excludes the detection of radicals also formed in flames. This sampling device is close to the one used by Grotheer et al. [12] for the study of sooting atmospheric pressure flames by photo ionization mass spectrometry (PIMS). They indeed used a similar fast sampling system (pressures in the sampling tube between 15 and 55 mbar) which also provides the advantage to suppress undesired reactions in the sampling line. The only difference with our system is that they use an additional He line connected to the sampling line in order to improved their molecular beam intensities.

Eventually, species to be measured by LIF are isentropically expanded into the analysis chamber through a nozzle aperture (1 mm orifice diameter) positioned at the center of the cylindrical chamber. The vertical position of the nozzle relative to the laser beam is precisely adjustable thanks to a micrometric translation stage.

2.3 Analysis chamber

This chamber has been described in detail in [8]. It consists of a cylinder equipped with three optical access windows, the inner wall of which is treated with a black coat of special paint (developed for space applications) in order to reduce the contribution to the signal from background scattering. Fluorescence is collected at 90° to the laser beam axis with a system of lens and mirrors placed as close as possible to the supersonic free jet in order to maximize the solid angle of collection. To generate this free jet, we use a turbomolecular pump (550 litres per second). The pressure of the gas sampled from the flame, i.e. the pressure before the nozzle, is maintained at a constant pressure of 10 torr by the use of a 25 m^3/h primary pump and is regulated by a motorized regulation valve. In these conditions, the pressure reached inside the chamber is around 5×10^{-3} torr. The naphthalene molecules are excited just a few millimeters under the nozzle.

2.4 Calibration procedure

The analysis chamber, where species are expanded to generate the supersonic jet, can independently be connected to either the low-pressure burner or to a glass container filled with a known concentration of naphthalene which allows the absolute calibration of the LIF signal coming from the probed molecules inside the free jet. Unlike benzene which is liquid and has a high vapor pressure, naphthalene is a solid powder in its standard state, characterized by a low vapor pressure (around 5×10^{-2} torr at 293 K) [10]. We therefore used a turbomolecular pump to empty the glass container in order to get a sufficient vacuum before filling it with naphthalene vapor. Under these conditions, a vacuum with a typical residual pressure of 10^{-4} torr could be achieved, i.e. two orders of magnitude lower than the naphthalene vapor pressure at ambient temperature. Commercially available naphthalene (Aldrich 99+%) was purified before sending its vapor inside the container according to the following classical protocol: (1) a specific amount of solid naphthalene is placed into a small reservoir, (2) the reservoir is placed in liquid nitrogen and thus drastically cooled down, and the residual vapor above the solid is pumped, (3) when the pressure no longer changes, the liquid nitrogen is removed and the pumping of the vapor phase is maintained until the solid naphthalene returns to ambient temperature. This procedure is repeated 3 times. Then the reservoir containing the naphthalene at ambient temperature is connected to the evacuated glass container. The vapor pressure of the purified naphthalene will thus fill the container until an equilibrium pressure is reached which corresponds to the saturated vapor pressure of the naphthalene at the temperature of the experiment. A typical curve relating the time evolution of the naphthalene vapor pressure inside the container is reported in Fig. 2. Then, after the pressure has reached a stable value and the system is well thermalized (which takes approximately 30 minutes according to Fig. 2) we fill the container with gaseous nitrogen to a total pressure of 1000 torr. The accuracy of the experimental protocol can be verified by comparing the saturated vapor pressure we obtained at 21°C, equal to $(5.57 \pm 0.05) \times 10^{-2}$ torr, to the one recommended by Ruzicka et al. [10] of 5.50×10^{-2} torr at the same temperature. So, thanks to this apparatus, we are able to generate a naphthalene mole fraction in the order of 55 ppm diluted

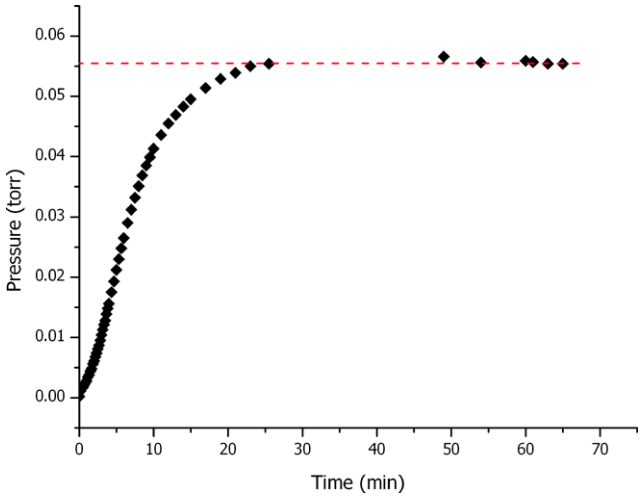

Fig. 2 Temporal evolution of the naphthalene vapor pressure filling the container

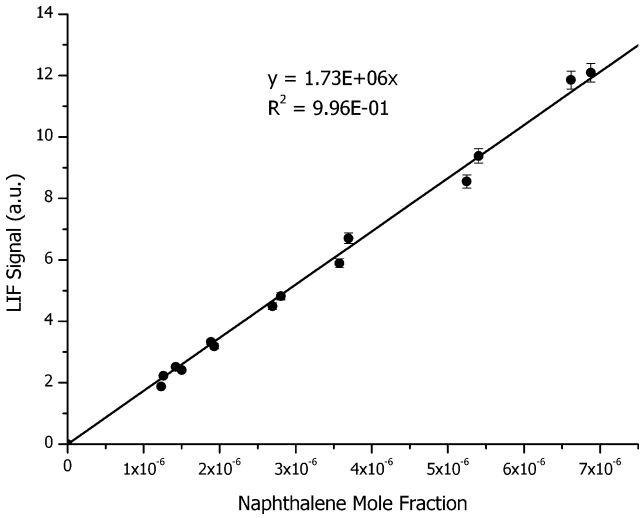

Fig. 3 Example of a calibration curve of the LIF signal

in N_2 inside the container. The Teflon line joining this container to the analysis chamber is coupled to another line carrying pure N_2 or a N_2–O_2 mixture and both gas flows are accurately regulated by two mass flow controllers (MFC) (see Fig. 1). This set-up thus enables the dilution of the naphthalene concentration sent into the analysis chamber and therefore allowed the calibration of the LIF signal. An example of such a calibration curve is shown in Fig. 3. We estimate an experimental accuracy of approximately 5% in the calibration of the signal determined by this procedure. Calibrations were always carried out after the measurements of concentration profiles of naphthalene in a flame. This minimizes the uncertainties linked to the comparison of LIF signals from the flame and from the calibration set-up by assuring the same conditions of wavelength, laser energy and optical arrangement for the collection of the fluorescence signal.

3 Results and discussion

The quantitative aspect of the jet-cooled fluorescence method is based on the calibration of the LIF signal from the naphthalene extracted from the flame by the LIF signal measured with known concentrations of pure naphthalene diluted in nitrogen or a N_2–O_2 mixture. The gaseous environment during the calibration is much less complex than the one of the naphthalene extracted from the flame. It is well known that the gas carrier used for supersonic jet generation can have an impact on the efficiency of the cooling of the jet, and therefore on the quantitative aspect of the method. Therefore we have carried out a study to check this point. We examined how the temperature and collision rates of the naphthalene evolved within the expanded free jets under various experimental conditions. This study, based on spectroscopic considerations, is presented in detail in the following sections.

3.1 Parametric study of the naphthalene spectroscopy under free jet conditions: Validation of the method for PAH mole fraction measurements

The naphthalene molecule is a planar molecule, near prolate asymmetric top of D_{2h} symmetry with an asymmetry parameter of $k = -0.68$ in the ground state. This molecule has been extensively studied spectroscopically [13–20]. Composed of 18 atoms, it has 48 normal modes of vibration among which 33 are in-plane and 15 are out-of-plane, all of them non-degenerate. We focused our work on the vibronic band reported in Fig. 4 located in the 308 nm spectral region, assigned as the $S_1A^1B_{1u} \leftarrow S_0X^1A_g$ transition, and more specifically on the intense transition near 308.2 nm, denoted as $44_0^1(b_{3g})$, which is characterized by a vibrational band origin at 32453.51 cm^{-1} [21]. It is important to note that the nomenclature of the vibrational modes in the literature is very confusing due to the different conventions followed according to the choice of the coordinate axis and mode numbering. In this paper, we will follow the axis notation according to the Mulliken convention [22] as used by Hollas et al. [23, 24], i.e. we will take the y-axis along the top axis (a-axis) of the molecule and the x-axis as normal to the molecular plane (c-axis). Hence the intense band of the spectrum reported in Fig. 4 and denoted in this paper $44_0^1(b_{3g})$ is the same as the one denoted $33_0^1(b_{2g})$ in [21, 25] or $\bar{8}_0^1(b_{1g})$ in [14, 15]. Conversions between the different conventions can be found in the paper of Joo et al. [25]. The choice of the present convention has been done in order to facilitate the comparison with the spectroscopic study of Hollas et al. [23, 24], which highlights some similarities with ours.

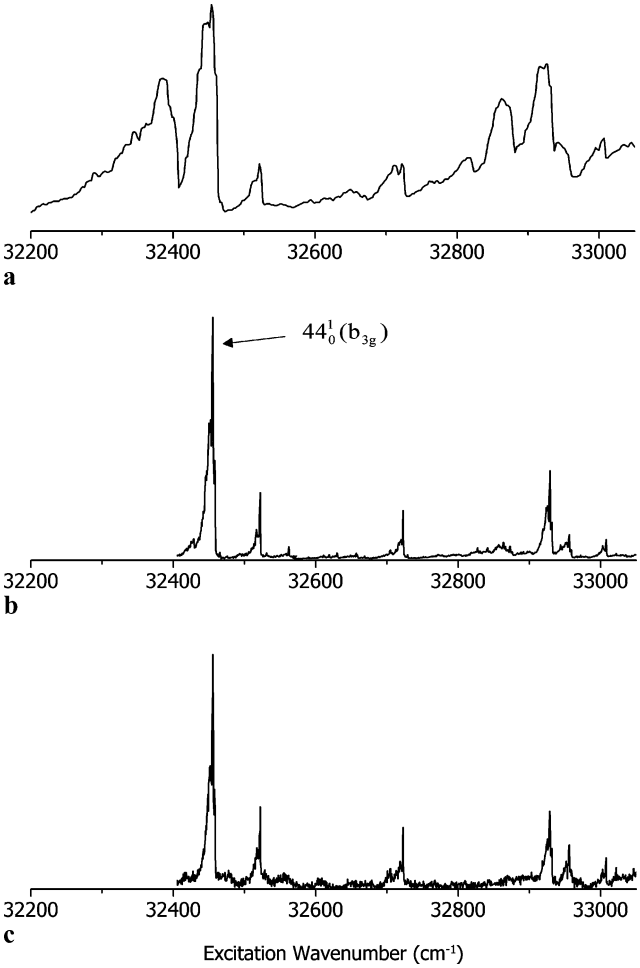

Fig. 4 Excitation spectra of naphthalene. (**a**) Room temperature naphthalene vapor at 5×10^{-5} torr (Behlen et al. [15]). (**b**) Naphthalene diluted in N_2 cooled in the supersonic jet (this work). (**c**) Naphthalene extracted from the flame cooled down in the supersonic jet (this work)

3.2 Temperature

The use of spectroscopic methods is generally obsolete for the selective measurement of species consisting of more than 4 atoms in flames because of the lack of spectral selectivity (unresolved spectra) under flame experiment conditions (temperature and pressure). The selectivity of the method presented here is provided by the drastic cooling of the molecules inside the supersonic free jet, which leads to the simplification of the electronic spectra of the molecules. This point is clearly highlighted in Fig. 4. Spectrum (a) corresponds to the one recorded by Behlen et al. [15] at room temperature and 5×10^{-5} torr, whereas spectra (b) and (c) have been recorded using our system, with pure naphthalene diluted in nitrogen and with naphthalene extracted from the flame ($\Phi = 2.32$) respectively. All the spectra have been normalized for a better comparison.

It is also important to note here that for the two spectra recorded with our experimental set-up the structure of all the experimental spectra are not significantly altered when the main gas carrier is changed from N_2 to the flame gaseous environment. Indeed, lineshapes and positions of the vibronic bands remain the same in both experiments. The slightly increased noise in spectrum (c) relative to spectrum (b) is due to a lower concentration of naphthalene. This indicates a comparable rotational and vibrational cooling, which is an important parameter for the accuracy of the calibration procedure based on a comparison of the signal intensities of naphthalene diluted in nitrogen and naphthalene sampled from the flame. Both rotational and vibrational temperatures can be extracted from the experimental spectrum of the naphthalene inside the supersonic free jet. For this purpose, we used the program *AsyrotWin* [26] with the spectroscopic data determined by Kabir et al. [21] to calculate the spectrum corresponding to the intense type B band 44^1_0 around 308 nm, which is reported in Fig. 5. This band is accompanied by a series of sequence bands which are characteristic of weak vibrational cooling. The identification of the sequence bands (labeling and positions) is based on their relative shifts in comparison with the origin band 44^1_0. We thus identified 4 more B type sequence bands $44^1_0\,24^1_1$, $44^1_0\,48^1_1$, $44^1_0\,48^1_1\,24^1_1$, $44^1_0\,48^2_2$, shifted respectively from -5.7, -9.9, -15.98 and -19.87 cm^{-1} from the origin band, which is very consistent with the work done by Hollas et al. [23, 24]. In this way, we found the best agreement between experimental and calculated spectra by adjusting the rotational temperature to 90 K and setting the intensities of the sequence bands equal to 0.17, 0.15, 0.06 and 0.03 relative to the origin band. These intensities $I(\nu_i)/I(\nu_{\text{Origin}})$ are directly equal to the vibrational Boltzmann factor $e^{-\frac{\nu_i}{kT_{\text{vib}}}}$ (with $k = 0.6952$ cm^{-1}/K). Therefore this enables the determination of the vibrational temperature T_{vib} of the corresponding modes ν_i [23, 27]. We calculated a temperature of 292 K for the in-plane vibration mode ν_{24} and 126 K for the out-of-plane vibration ν_{48}. This confirms previous conclusions that there is a greater propensity for vibrational cooling of the out-of-plane vibrations than for in-plane ones [15, 23, 24]. The fact that we found a moderate vibrational temperature for the ν_{24} mode is due to the relatively low pressure of the gas carrier within our experimental set-up (only 10 torr of sampling) used to generate the supersonic free jet, which is not enough to promote a drastic vibrational cooling. Nevertheless, as is shown in the next part of the paper, this vibrational cooling is adequate to obtain sufficient spectral resolution to allow a selective detection of the naphthalene extracted from the flame. Finally, it is noteworthy that the rotational temperature of 90 K determined here is equal to the one previously calculated for the benzene molecule under similar experimental conditions. Both the low rotational and vibrational temperatures are mainly explained by the thermalization of the species to 373 K before their supersonic expansion. Without this initial temperature decrease of the

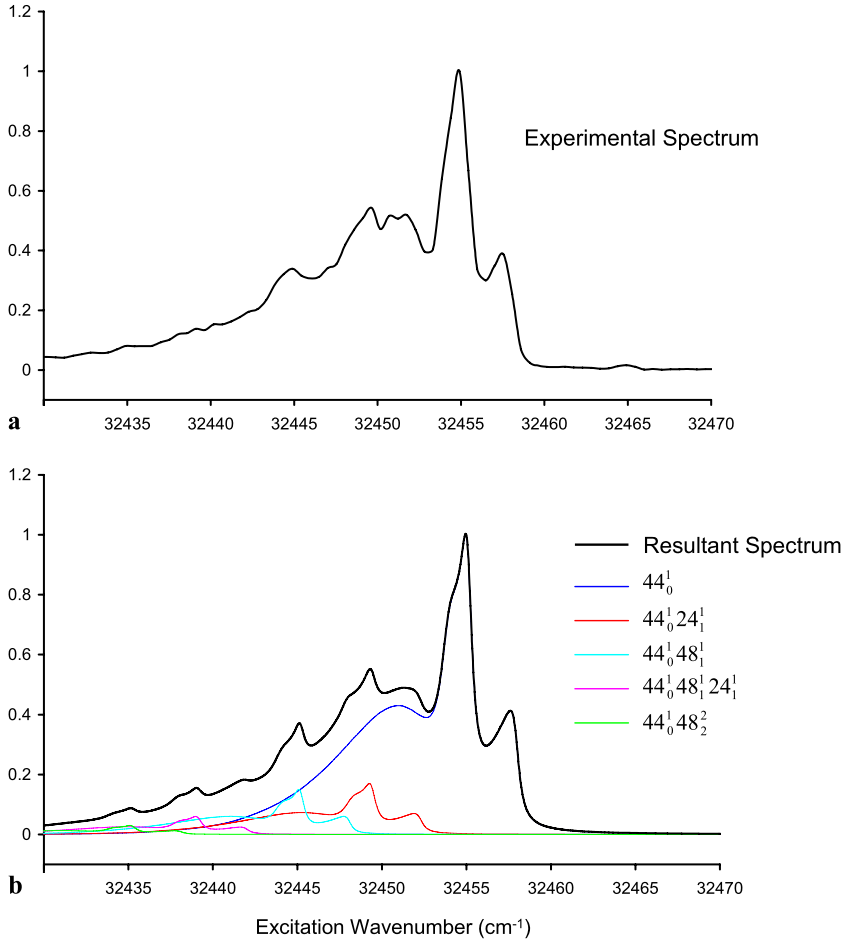

Fig. 5 Comparison between the experimental spectrum (**a**) of naphthalene recorded in the region of the 44^1_0 band and the computed spectrum (**b**) at a rotational temperature of 90 K by considering 4 additional sequence bands

gases sampled from the flame, it would have been extremely difficult to achieve adequate rotational cooling. This point has been previously noted by Kamphus et al. [28] who determined rotational temperatures between only 240 to 440 K in the molecular beam of their MBMS instrument (Molecular Beam Mass Spectrometry) coupled to a low-pressure flame.

3.3 Selectivity of the method

The selectivity of the method is directly related to the spectral selectivity. The efficiency of the cooling, which has already been discussed, is the key point to avoid spectral interferences between sampled species. Nevertheless, the spectroscopic properties of the PAH as well as the thermalization of the species before their analysis are also important.

The spectroscopy of PAH is governed by the Kasha's rule, i.e., the fluorescence spectrum is always shifted to higher wavelengths compared to the excitation. So we have a dual spectral selectivity, as the excitation wavelength and the fluorescence collection spectral range are very specific to each species under jet-cooled conditions and both require to be precisely adjusted. Furthermore, PAH spectroscopy in the UV-visible range relies on the HOMO-LUMO transitions from a bonding π orbital to an anti-bonding π^*. Increased conjugation, linked to the increased size of PAH, brings the HOMO and LUMO orbitals closer together and so shifts the absorption bands to longer wavelengths. This property, associated with the resolved structure of PAH spectra, offers a second limitation to the possibility of PAH spectral interference.

The other point concerns the heated sampling line which was required to transport the species from the burner to the analysis chamber. As already stated, this device restricts the detectable species to the stable ones. However, this limitation provides two specific advantages. First, by preventing radical species formed in the flame being sampled by the microprobe it reinforces the selective feature of the set-up by avoiding the simultaneous excitation of these species with the PAH, and thus possible interferences of the measured PAH fluorescence signal. A second crucial aspect of the sampling line is that the species are thermalized to a few hundred Kelvin before their supersonic expansion. As previously discussed, this feature was essential in providing an efficient rotational and to a lesser extent vibrational cooling

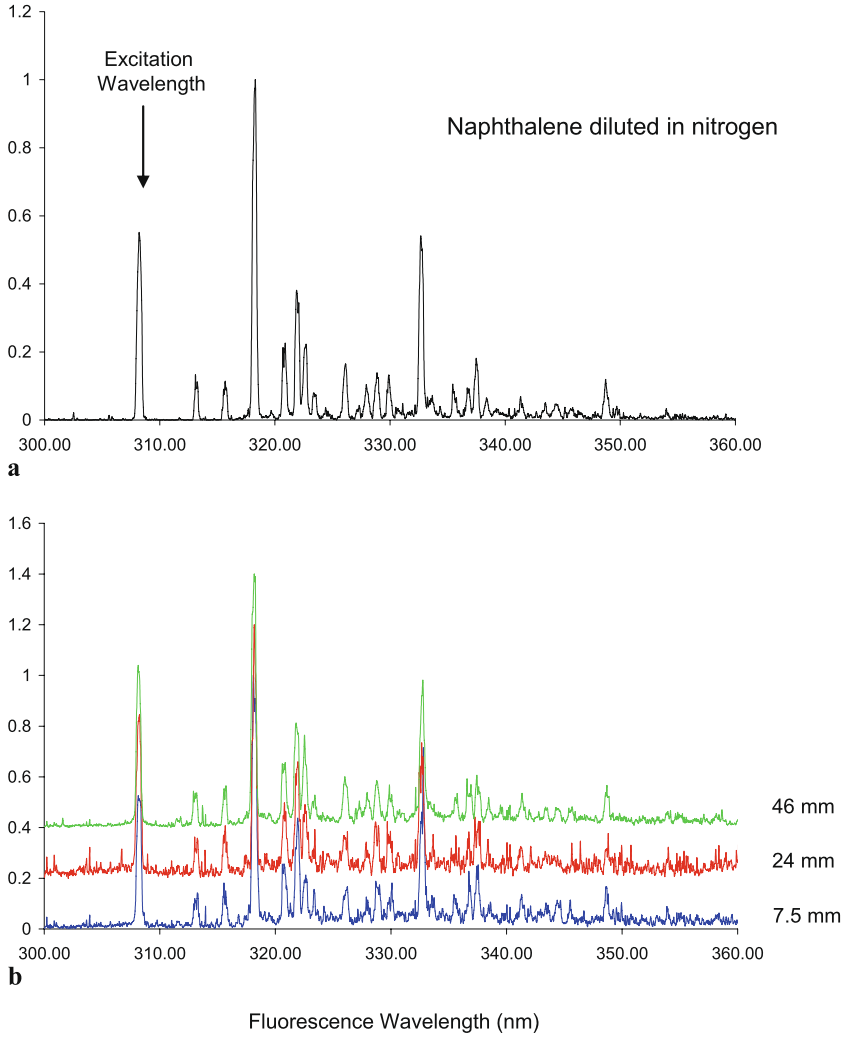

Fig. 6 Fluorescence spectra of the naphthalene from 44_0^1 excitation for (**a**) pure naphthalene diluted in N_2 and (**b**) naphthalene sampled at different heights above the burner in the sooting flame ($\Phi = 2.32$)

of the species and therefore a good spectral selectivity of the method.

So, considering that only red shifted, fluorescing, stable species formed in flames and absorbing in the UV–visible spectral range can be detected, the present set-up is especially well adapted in terms of spectral selectivity for PAH detection.

The selectivity of the method has essentially been checked by studying the structure of the emission fluorescence spectra of the naphthalene issued from different heights above the burner. Figure 6 shows the normalized fluorescence spectra obtained for a mixture of naphthalene diluted in nitrogen (after excitation of the $44_0^1(b_{3g})$ transition, near 308.2 nm) and in a sooting flame ($\Phi = 2.32$). The spectra acquired from the flame have been measured at three different heights above the burner, 7.5 mm (peak of naphthalene profile), 24 mm and 46 mm (sooting zone in the burnt gases) respectively. The baselines of the spectra have been vertically shifted for a better comparison. We observe sharp and structured spectra, easily assignable, with intensities in excellent agreement with the ones measured in [13] for the same excitation wavelength in a supersonic jet experiment (pure naphthalene diluted in He). By comparison with the pure naphthalene spectrum, we did not observe any spectral interference nor any structural change of the fluorescence emission spectrum all along the flame height. The unchanged structure of these spectra also confirms the absence of any laser-induced incandescence (LII) feature coming from soot particles, which could have potentially been observed for the sooting part of the flame. This is further confirmed by the absence of visible broadband signal when tuning the laser off resonance. The selectivity of the method therefore appears to be excellent, allowing the careful measurements of PAH in flames.

3.4 Collision rate and fluorescence decay times

The last important point of the calibration procedure that needs to be checked is the collision rate of the naphthalene inside the expanded free jet. This is crucial as the experimental measurements are determined from the temporally

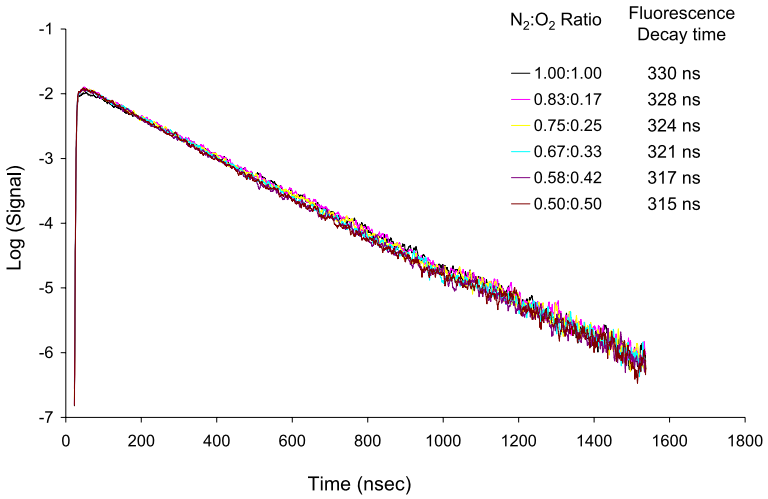

Fig. 7 Semilogarithmic plot of the naphthalene fluorescence decays for several N_2–O_2 ratios used as gas carrier

integrated LIF signal and thus directly dependent on the fluorescence lifetime. A systematic study has been carried out in order to determine the sensitivity of the naphthalene fluorescence lifetime to its gaseous environment under our jet experimental conditions. We more particularly checked the influence of the O_2 concentration on the quenching of the naphthalene fluorescence. We have first performed a series of measurements of the fluorescence decay times of naphthalene diluted in different mixtures of N_2–O_2 from 1:0 to 0.5:0.5. The lifetimes have been determined by fitting the decay signals with a procedure based on a nonlinear algorithm for mono-exponential signals. No long temporal component has been observed for any of these signals, with all decay curves being purely monoexponential. The semilogarithm plot of all the experimental signals as well as the corresponding fluorescence decay times are reported in Fig. 7. From these measurements, it appears that under the conditions of our supersonic jet oxygen has only a very small measureable influence on the fluorescence decay time. We observe a maximum decay time of 330 ns for the naphthalene diluted in pure N_2 and a decrease of 4.5% (315 ns) in the N_2–O_2 $(0.5:0.5)$ mixture. These values (315 to 330 ns) are closed to the ones reported in the literature for this specific excitation wavelength. Indeed, under low-pressure conditions (vapor phase), Stockburger et al. [18] and Ohta et al. [29] measured lifetimes around 270 and 275 ns respectively. Behlen et al [16] determined a zero-pressure fluorescence lifetime of 317 ± 10 ns under supersonic jet conditions. More recently, Martinez et al. [30] investigated naphthalene fluorescence quenching by O_2, N_2 and H_2O. They did not observe any significant quenching with H_2O at the limit of their experimental mixing ratio (3.5%). Besides, they clearly highlighted a more significant contribution of O_2 in comparison with N_2 to the quenching of the naphthalene fluorescence. From these measurements, they extrapolated a zero-pressure fluorescence decay time of 340 ± 10 ns. Our values are in good agreement with those determined by Behlen and Martinez and according to the reported experimental uncertainties, confirm the near zero collision conditions provided by our set-up. The influence of the O_2 concentration on the fluorescence decay time, although detectable, is much less critical in our case due to the supersonic jet conditions and the resulting reduced collisions.

Table 1 Experimental flames conditions

	CH_4	O_2	N_2	Eq. Ratio
Flame 1	46%	40%	14%	2.32
Flame 2	45%	42%	15%	2.05
Flame 3	41%	45%	14%	1.82
Pressure	200 torr		Total Flow Rate	3.96 l/min STP

From the determination of these temporal signals, we can estimate the variation of the corresponding temporal areas relative to the different gaseous environments of the naphthalene. The area under the temporal LIF signal, for the same concentration of naphthalene, has been calculated to decrease by only 3% when the concentration of oxygen was increased from 0 to 50% of the total gas carrier. This parameter can thus be considered as a very minor source of error for the measurement of the naphthalene concentration.

Another series of fluorescence lifetime measurements have been made with naphthalene sampled from the flame at three different heights above the burner of 7.5, 24 and 46 mm. The normalized fluorescence signals are reported in Fig. 8. The corresponding decay times are 322, 326 and 326 ns. These measurements are therefore very consistent with the fluorescence decay times previously determined for pure naphthalene diluted in different N_2–O_2 mixture. Moreover, we note a variation of only 2% of the decay time all along the flame height, which suggests a very weak impact on the quenching of the naphthalene fluorescence by the gaseous environment of the flame.

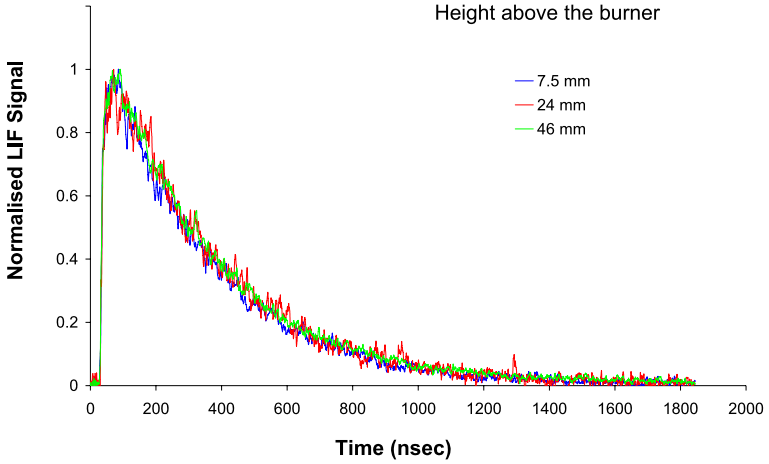

Fig. 8 Normalized temporal fluorescence decays signals of naphthalene recorded at different heights above the burner in the sooting flame ($\Phi = 2.32$)

The result of the above attests both the quantitative aspect of the method and the accuracy of the calibration procedure of the LIF signals to get PAH concentration profiles in flames.

4 Application of the method for the measurements of the naphthalene profiles in flames

In this last part we report experiments performed using this method in low-pressure flames. Our goal here is not to provide a detailed chemical analysis of the flame structure but only to show the capacities of the method for flame studies. Hence, we have recorded quantitative mole fraction profiles of naphthalene in three different rich flames stabilized at 200 torr and characterized by various equivalence ratios from 1.82 to 2.32. Experimental conditions are reported in Table 1. The critical equivalence ratio above which flames produce soot particles has been visually determined at around 2.05. Therefore flames with an equivalence ratio of 1.82, for which no yellow emission was discernable, have been considered as non-sooting flames and flames with equivalence ratio of 2.05 and 2.32 as sooting. It is to be noted that this threshold is confirmed by experiments carried out by laser-induced incandescence (LII). No LII signals were recorded for flames with an equivalence ratio lower than 2.05.

The experimental concentration profiles of naphthalene are reported in Fig. 9. Each of them is the result of the average of several experimental profiles. Error bars correspond to the experimental statistical errors. From the inset of Fig. 9, which corresponds to the naphthalene profile determined in the flame at $\Phi = 1.82$, we have estimated a detection limit of the order of 1 ppb under flame conditions. The uncertainties of the measurements can be partly attributed to the calibration procedure, but principally to the accuracy and reproducibility of the probe position vs. the flame height. This last point is clearly highlighted by the increase of the error bars when the concentration gradient is sharp. In addition, the region of the flame which is far from the burner surface (burnt gases) may be subject to small fluctuations, which are a supplementary source of experimental uncertainties. From all these measurements, we obtained an average uncertainty for the experimental measurements of approximately $\pm 10\%$.

With respect to the profiles, it is worth noting that they all highlight a global shape similar to the previous benzene profiles we measured in the same flames and already discussed in [8]. That is, they can be separated into 3 different regions each associated with a different chemical process. The first zone is where only gaseous reactions take place leading to the rapid formation of the naphthalene. This zone is present from approximately the burner surface up to 7 mm. There is then a second region where the naphthalene is consumed up to a minimum threshold. This region is the zone where soot begins to form for the 2 sooting flames (approximately 10 mm for both flames). Finally there is a third region, which can be regarded as a pyrolysis reaction zone where the naphthalene mole fraction continuously increases with height above the burner. The increase of the naphthalene concentration is much more pronounced for flame 1 ($\Phi = 2.32$) than for flame 3 ($\Phi = 1.82$), which was also observed in [8] with benzene formation. The shape of the naphthalene profiles are highly similar to those of benzene that we measured previously, the first peak mole fraction of naphthalene, for the 3 flames, all being shifted by 1 mm downstream the flame.

Moreover, we also observed a strong dependence of the measured mole fraction of these first peaks according to equivalence ratio. We determined a mole fraction of 2.5×10^{-6} for flame 1 ($\Phi = 2.32$), 6×10^{-7} for flame 2 ($\Phi = 2.05$) and 6.1×10^{-8} for flame 3 ($\Phi = 1.82$). We have characterized the dependence of the naphthalene formation on the equivalence ratio according to the empirical law $X_i = A_i \Phi^{ni}$ as proposed by Melton et al. [4, 6]. X_i corresponds to the mole fraction of the naphthalene at the first

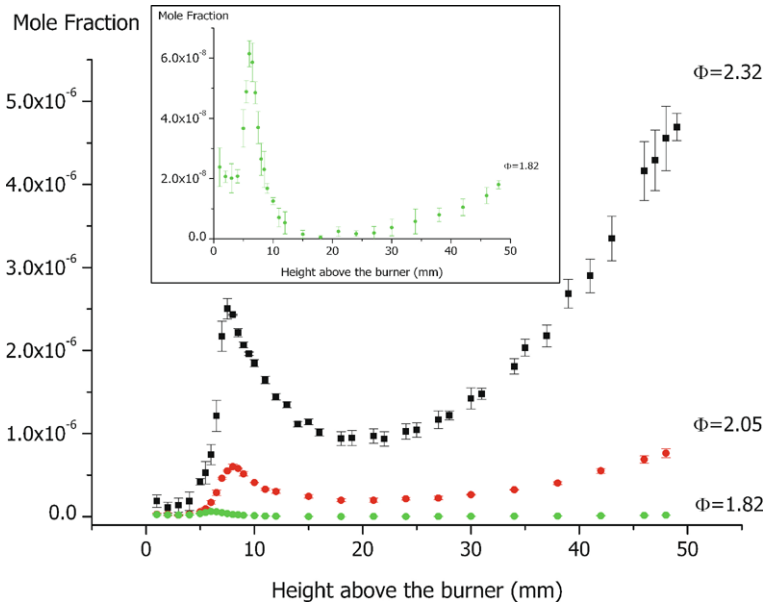

Fig. 9 Naphthalene mole fraction profiles determined in three flames characterized by equivalence ratios of 2.32, 2.05 and 1.82

peak of the profile, Φ is the equivalence ratio, and A_i and ni are correlation parameters. The term ni represents the sensitivity of X_i to the equivalence ratio. In our flame conditions, the measured mole fractions at the first peak of the profiles reveal a dependence of the naphthalene formation on the equivalence ratio that we can fit with the empirical law as $X_{\max} = 7.6 \times 10^{-12} \cdot \Phi^{15.2}$. The value of ni (15.2) determined is greater than the one we found previously [8] for benzene ($ni = 11.6$) denoting a higher sensitivity to the equivalence ratio for the naphthalene, as also observed at atmospheric pressure by Melton et al. [6].

5 Conclusion

In this paper, we have demonstrated the interest of the jet-cooled LIF method for the quantitative measurement of naphthalene profiles in flames. The technique has been shown to be very selective and especially well designed for PAH measurements in flames. The spectral selectivity is mainly due to the use of a thermalized sampling line, which, after sampling of the species from the flame with a microprobe, enables efficient rotational cooling and a drastic simplification of the excitation molecular spectra. A number of experiments have been carried out in order to establish the quantitative aspect of the method and to check for the influence of various parameters on this feature. The main potential source of error which has been attributed to the evolution of the gaseous environment of the naphthalene species, according to the flame height, has been shown to have only a very weak impact on the accuracy of the measurements.

From measurements made in three different methane flames, this technique has been proved to enable the determination of accurate, reproducible and spatially-resolved concentration profiles of naphthalene under non-sooting or sooting flame conditions. The detection limit has been estimated for naphthalene to be 1 ppb. Furthermore, the accuracy of the method has been shown not to be affected by the presence of soot in the flame. The only requirement in this case is to enlarge the orifice of the microprobe in order to avoid it clogging. From the measurement of naphthalene profiles in different rich flames stabilized at low pressure, we observe a high sensitivity of the naphthalene formation according to the equivalence ratio, as has already been reported for the same kind of studies at atmospheric pressure.

Finally, we would like to conclude with the potential of this relatively simple set-up for the direct measurements of higher molecular weighted PAH. The main problem with the analysis of these compounds with probe sampling methods concerns their condensation along the sampling line, which usually requires strong heating of the line. Here, samples of only 10 torr of pressure are required for the analysis. This should allow for the detection of higher number-member rings PAH (as pyrene) having very low vapor pressure and open the way for providing challenging data for the understanding of PAH formation in flames.

Acknowledgements The CERLA (FR CNRS 2416) is supported by the French Research Ministry, the Nord–Pas de Calais Region and the European Funds for Regional Economic Development. This work was supported by the Air Quality Program of IRENI (Institut de Recherche en ENvironnement Industriel) and the Agence Nationale de la Recherche (ANR-Contract 06-BLAN-0349).

References

1. H. Richter, J.B. Howard, Prog. Energy Combust. Sci. **26**, 565 (2000)

2. M. Frenklach, Phys. Chem. Chem. Phys. **4**, 2028 (2002)
3. B. Apicella, R. Barbella, A. Ciajolo, A. Tregrossi, Combust. Sci. Technol. **174**, 309 (2002)
4. T.R. Melton, F. Inal, S.M. Senkan, Combust. Flame **121**, 671 (2000)
5. P. Desgroux, X. Mercier, B. Lefort, R. Lemaire, E. Therssen, J.F. Pauwels, Combust. Flame **155**, 289 (2008)
6. T.R. Melton, A.M. Vincitore, S.M. Senkan, Proc. Combust. Inst. **2**, 1631 (1998)
7. F. Liu, K.A. Thomson, H. Guo, G.J. Smallwood, Combust. Flame **146**, 456 (2006)
8. X. Mercier, M. Wartel, J.F. Pauwels, P. Desgroux, Appl. Phys. B, Lasers Opt. **91**, 387 (2008)
9. The McKenna Flat Flame Burner, Holthuis & Associates, P.O. Box 1531, Sebastopol, CA 95473
10. K. Ruzicka, M. Fulem, V. Ruzicka, J. Chem. Eng. Data **50**, 1956 (2005)
11. V. Oja, E.M. Suuberg, J. Chem. Eng. Data **43**, 486 (1998)
12. H.-H. Grotheer, K. Hoffmann, K. Wolf, S. Kanjarkar, C. Wahl, M. Aigner, Combust. Flame **156**, 791 (2009)
13. S.M. Beck, J.B. Hopkins, D.E. Powers, R.E. Smalley, J. Chem. Phys. **74**, 43 (1981)
14. S.M. Beck, D.E. Powers, J.B. Hopkins, R.E. Smalley, J. Chem. Phys. **73**, 2019 (1980)
15. F.M. Behlen, D.B. McDonald, V. Sethuraman, S.A. Rice, J. Chem. Phys. **75**, 5685 (1981)
16. F.M. Behlen, S.A. Rice, J. Chem. Phys. **75**, 5672 (1981)
17. H. Gattermann, M. Stockburger, J. Chem. Phys. **63**, 4541 (1975)
18. M. Stockburger, H. Gattermann, W. Klusmann, J. Chem. Phys. **63**, 4529 (1975)
19. K. Yoshida, Y. Semba, S. Kasahara, T. Yamanaka, M. Baba, J. Chem. Phys. **130**, 194304 (2009)
20. W. Majewski, W.L. Meerts, J. Mol. Spectrosc. **104**, 271 (1984)
21. M.H. Kabir, S. Kasahara, W. Demtroder, Y. Tatamitani, A. Doi, H. Kato, M. Baba, J. Chem. Phys. **119**, 3691 (2003)
22. R.S. Mulliken, J. Chem. Phys. **23**, 1997 (1955)
23. J.M. Hollas, T. Ridley, P.A. Freedman, Chem. Phys. Lett. **92**, 317 (1982)
24. J.M. Hollas, S.N. Thakur, Mol. Phys. **22**, 203 (1971)
25. D.-L. Joo, R. Takahashi, J. O'Reilly, H. Katô, M. Baba, J. Mol. Spectrosc. **215**, 155 (2002)
26. R.H. Judge, D.J. Clouthier, Comput. Phys. Commun. **135**, 293 (2001)
27. V.A. Walters, D.L. Snavely, S.D. Colson, K.B. Wiberg, K.N. Wong, J. Phys. Chem. **90**, 592 (1986)
28. M. Kamphus, N.-N. Liu, B. Atakan, F. Qi, A. McIlroy, Proc. Combust. Inst. **29**, 2627 (2002)
29. N. Ohta, H. Baba, J. Chem. Phys. **76**, 1654 (1982)
30. M. Martinez, H. Harder, X. Ren, R.L. Lesher, W.H. Brune, Atmos. Chem. Phys. **4**, 563 (2004)